

ORIGINAL PAPER  
ΕΡΕΥΝΗΤΙΚΗ ΕΡΓΑΣΙΑ

**Lung edema and thrombosis induced by activated mannose-binding lectin-associated serine protease 2 and MHC class I reactions, and liver thrombosis aggravated by suppressed phosphotyrosine and female donor reactions to male-specific antigens in Lewis rats**

**OBJECTIVE** The causes of lung edema and thrombosis and liver embolism were investigated in rats. **METHOD** Lewis rats were used. Mannose-binding lectin (MBL)-associated serine protease 2 (MASP-2) antibody (Ab) was injected to cause lung edema. Lung and liver thrombosis and embolism were generated using major histocompatibility complex (MHC) class I monoclonal Ab (mAb) and MASP-2 Ab. Liver embolisms and male-specific antigen reactions of minor histocompatibility antigens (mHA) were triggered by phosphotyrosine (pTyr) mAb. Correlative expressions of MASP-2 and pTyr were confirmed by flow cytometry (FCM). **RESULTS** MASP-2 Ab caused acute intraalveolar and peribronchovascular edema, which was characterized by hemolytic red cell casts, type II cell activation with lamellar body (Lb) secretion and elevated apocrine secretion of Clara cells. MHC class I mAb and MASP-2 Ab caused severe lung and liver thrombosis and embolism. Immunohistochemically stained electron micrographs of alveolar type I cells showed a quick-activation of the second MASP-2, when the first MASP-2 was destroyed by MASP-2 Ab. In the liver injected with pTyr mAb, hepatocytes underwent selective apoptosis with Golgi apparatus disturbances. Liver thrombosis, which was aggravated by female donor immune rejections of male-specific mHA, was associated with hepatic venous dilatation. Heparin sodium accelerated lung surfactant (Lb) secretion. Exogenous chemotactic inhibitor suppressed cytokine-induced chemokines, which were triggered by pTyr mAb. **CONCLUSIONS** Lung edema and thrombosis were caused by MASP-2 and MHC class I Abs. pTyr mAb injection accelerated liver thrombosis, based on tyrosine kinase disturbances, in which mHA immune reactions aggravated liver thrombosis.

Mannose or mannan-binding lectin (MBL)-associated serine protease 2 (MASP-2) belongs to a serine protease family that mediates proteolytic cascades of complement (C), coagulation and fibrinolysis systems. MASP-2 encompasses 2 complement control protein modules (CCP) and a serine protease (SP) domain. MASP-2 dimer functions, as well as the much larger C1<sub>r2</sub>-C1<sub>s2</sub> tetramer in the C1 complex of the classical pathway through different sets of enzyme-substrate interactions.<sup>1</sup> MASP-2 cleaves C2 and C4. Spontaneous hydrolysis of C3 is initiated by MASP-2. MBL

binds to carbohydrate enzyme on the surface of pathogens, and triggers the complement cascade through MASP-2 leading to opsonization. These complement cascades through MASP-2 are associated with innate immune reactions. MASP-2 also promotes fibrinogen turnover after prothrombin is cleaved to thrombin.<sup>2</sup> The activated thrombin splits factor XIII and fibrinogens, and activates platelets.

Stimulation of protein tyrosine kinase results in production of phosphotyrosine (pTyr). Receptor tyrosine kinases (RTK) are important in many biological functions, including

ARCHIVES OF HELLENIC MEDICINE 2011, 28(5):680-691  
ΑΡΧΕΙΑ ΕΛΛΗΝΙΚΗΣ ΙΑΤΡΙΚΗΣ 2011, 28(5):680-691

**T. Nakatsuji**

*Department of Transfusion Cell Therapy,  
Hamamatsu University School of  
Medicine, Hamamatsu 431-3192, Japan*

Πνευμονικό οίδημα και θρόμβωση που προκαλούνται από ενεργοποίηση αντιδράσεων με MBL σε συνδυασμό με MASP-2 και αντιδράσεων του MHC τάξης I, καθώς και ηπατική θρόμβωση προκαλούμενη από αντιδράσεις καταστολής της φωσφοτυροσίνης σε θήλιες δότες και ειδικά αντιγόνα σε άρρενες αρουραίους Lewis

*Περίληψη στο τέλος του άρθρου*

**Key words**

Liver embolism  
Lung edema  
Lung thrombosis  
Mannose-binding lectin (MBL)-associated serine protease 2  
Tyrosine kinase

*Submitted 6.6.2011*

*Accepted 20.6.2011*

the immune systems. The Ron receptor is a multifunctional RTK which modulates inflammatory responses to hepatic injury.<sup>3</sup> Mouse Ron mRNA of 1.9 kb short-form Ron (SF-Ron) and 4.8 kb full-length Ron (FL-Ron) has been identified in hematopoietic stem cells. Solely expressed FL-Ron (but not SF-Ron) mice are reported to have produced a significant increase in interferon- $\gamma$  (IFN- $\gamma$ ) in splenocytes and to have exhibited worsened liver histology. It has also been reported that the phosphorylation of a tyrosine residue in  $\beta$ -catenin is associated with cell migration.<sup>4</sup> Down-regulation in the tyrosine phosphorylation of E-cadherin- $\beta$ -catenin complex led to down-regulation of the intracellular signaling pathway.

In this study using Lewis rats, it was shown that lung edema was induced by MASP-2 and pTyr activation, and pTyr suppression aggravated female donor bone marrow (BM) cell reactions to male hosts. The finding of multiple hemolytic red cell casts was an indicator of the lung edema. Major histocompatibility complex (MHC) class I monoclonal antibody (mAb) together with MASP-2 Ab, and male-specific antigens of minor histocompatibility antigens (mHA) together with pTyr mAb, aggravated thrombosis and embolism in the lung and liver. Both MASP-2 and pTyr Abs were associated with a hypercoagulability response. MASP-2 antigen destroyed by MASP-2 Ab was recovered quickly by activation of another MASP-2 antigen. As a result, expression of MASP-2 and pTyr was correlatively activated by MASP-2 Ab, but pTyr and MASP-2 were correlatively suppressed by pTyr mAb.

## MATERIAL AND METHOD

### Animals

Lewis (LEW/SsN) rats were purchased from Japan SLC Co Ltd (Hamamatsu, Japan). Secondly generated rats, which were born from sibling mothers and the same father, were used in this experiment. They were maintained in the animal center of Hamamatsu University School of Medicine. During their maintenance, microorganism infection was monitored using 2 decoy rats, which were maintained in the same room as the experimental rats. The monitored microorganisms were the hemagglutinating virus of Japan, mouse hepatitis virus, *Mycoplasma pulmonis*, and *B. piliformis*. The results for all of these organisms were negative. The experimental rats were bred and maintained in a clean room.

### Experiment designs

This experiment consisted of 6 different systems, classified into experiments (Exps) A, B, C, D, E and F. The detailed experimental designs are summarized in table 1. These experiments were started using the rat hosts at the ages of 8.1–9.0 weeks. At

the time of sacrifice, the body weights (BW) of the experimental female and male rats had increased from 164 $\pm$ 5 g to 173 $\pm$ 3 g and from 252 $\pm$ 3 g to 286 $\pm$ 14 g, respectively. Exp F males, which were planned to exhibit graft versus host (GvH) reactions, had BW of 236 $\pm$ 4 g at the starting age of 8.1 weeks and 286 $\pm$ 14 g at the sacrifice age of 10.8 weeks. Exp C, E and F rats were injected subcutaneously with heparin sodium (Novo Heparin) at a dose of 30 units per rat. Exp C rats were injected with heparin 4 times during 3 subsequent days. Exp E and Exp F rats were injected with heparin 6 times during 7 subsequent days. Rabbit polyclonal antibody (Ab) (IgG) of mannose or mannan-binding lectin (MBL) associated serine protease 2 (MASP-2) were purchased from Santa Cruz Biotechnology, Inc (CA, USA, www.scbt.com). MASP-2 Ab was raised against amino acids 260–344 mapping within an internal region of mouse origin MASP-2. Monoclonal antibody (mAb) (IgG1) of MHC class I was raised against rat class I MHC antigens (RT-IA) to recognize only a subfraction of the total class I MHC molecules (Sera Laboratories International, Ltd, West Sussex, England). Purified mouse anti-phosphotyrosine (pTyr) mAb (IgG2a) had reactivity to human and was tested in mouse, rat, chicken, dog and frog (BD Biosciences, Tokyo, Japan). Chemotactic inhibitor had the structure of N-Boc-Phe-D-Leu-Phe-D-Leu-Phe-OH (Bachem California, Torrance, CA, USA).

### Histopathological examination

From each rat, at least a quarter of the lung tissue, 1–1.5 cm $\times$ 0.8–1 cm-sized pieces of liver, a segment of ileum of 1 cm in length taken from 1 cm above the cecum, and a quarter of the spleen were fixed in 10% formalin (Sigma-Aldrich, St Louis, MO, USA) and stained with hematoxylin-eosin (H-E) for light microscopic examination. Samples from 7 untreated control females (Cont F) and 9 control males (Cont M) were also examined in the light microscopic analysis. A BX51 light microscope with a DP72 digital camera was used for light micrographs. For transmission electron microscopic (TEM) analysis, samples of Exp A-2 lung, Exp B-3 lung and Exp F-2 liver were selected. Immunochemical stain was applied before fixing in 2% glutaraldehyde for the detection of MASP-2 antigen or pTyr antigen. Lung samples from Cont F3, Exp C-3 and Exp D-2 and bone marrow (BM) from Exp D-3 were selected for immunochemical staining. A lung cell suspension of Cont F3 was divided into two parts. Apart from pTyr detection using the divided lung cell suspension from Cont F3, all the 4 kinds of cell suspensions described above were stained for MASP-2 detection. MASP-2 polyclonal Ab (Santa Cruz Biotechnology Inc) and pTyr mAb (BD Biosciences) were labeled with 15 nm gold colloidal particles (EY Laboratories, Inc, San Mateo, CA, USA) as pre-fixing procedures as described previously.<sup>5</sup> A JEM 12000 TEM (JEOL, Tokyo, Japan) was used to take transmission electron micrographs.

### Flow cytometer (FCM) analysis

One million mononuclear cells (MNC) were obtained from mesenteric lymph node (MLN), BM and lung tissue of all the experimental rats. MLN cell suspensions were stained with both

**Table 1.** The treatment summaries applied to the six groups of experimental rats, A, B, C, D, E and F.

Exp no (n <sup>†</sup> )	Sex	Antibody			CI*	BM cell** (×10 <sup>7</sup> /rat)	Observation (day)
		MASP-2	MHC <sup>‡</sup>	pTyr			
A (4)	F	4 µg	–	–	–	–	0.5–1
B (5)	M	4 µg	10 µg	–	–	–	0.5–1
C (4) <sup>§</sup>	M	5 µg	–	–	–	–	3
D (4)	F	–	–	15 µg	–	–	0.5–1
E (4) <sup>¶</sup>	F	–	–	20 µg	+	–	18
F (5) <sup>¶</sup>	M	–	–	20 µg	+	2	16

\*Chemotactic inhibitor (150 µg/rat), \*\*Female rat BM cells, <sup>†</sup>Total rat number, <sup>‡</sup>Class I (RT-IA) mAb, <sup>§</sup>Heparin sodium (30 units/rat) was injected MASP-2: Mannose-binding lectin (MBL)-associated serine protease 2, MHC: Major histocompatibility complex, pTyr: Phosphotyrosine, BM: Bone marrow

fluorescein-isothiocyanate (FITC) anti-rat CD3 mAb (Cedarlane Laboratories Ltd, Hornby, Ontario, Canada), which recognizes a rat T cell surface antigen located in the periarterial lymphatic sheaths of the spleen, and FITC anti-rat CD8a mAb, which mediates GvH disease in rats (Cedarlane Laboratories Ltd). All the cell suspensions of MLN were incubated with FITC-conjugated mAb for 30 minutes at 4° C. BM cell suspensions were stained with MASP-2 polyclonal Ab (Santa Cruz Biotechnology, Inc), and pTyr mAb (BD Biosciences) for 30 minutes at 4° C, both of which were double-stained with monoclonal mouse IgG1/FITC (Ansell Co, Bayport, MN, USA) for 15 minutes at 4° C. Lung cell suspensions were stained with MASP-2 Ab-FITC in the same way as BM cells. The stained MNC were assayed for their labeled FITC using an EPICSR XL-MCL system III FCM (Beckman Coulter, Fullerton, CA, USA). For the interpretation of MASP-2- and pTyr-positive cells, a fixed point between negative and positive peaks was used, as shown in figures 6a and 6b, because many results did not show a separate negative peak. The percentage of positive cells is presented as mean±standard deviation (M±SD), calculated by the Excel function of STDEVPA.

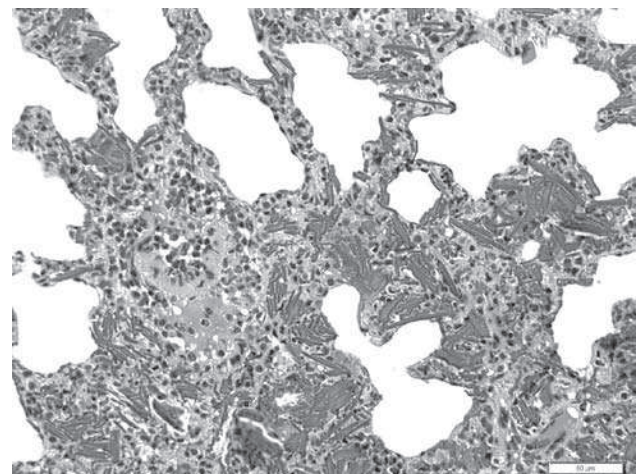
## RESULTS

Table 2 shows a summary of the pathological findings found in the Exp A to Exp F rats. As shown in table 1, Exp A to Exp C rats were given MASP-2 Ab, which caused lung edema. The lung edema of an Exp A-1 female is shown in figure 1a where many of hemolytic red cell casts can be observed along with eosinophils infiltrating the arterioles. Small red cell fragments are present around the casts. Hemolytic red cell casts, composed of both hemolytic red cells due to complement activation and red cell aggregation due to hypercoagulability, indicate MASP-2 activation induced by MASP-2 Ab. The lung edema shown by the red cell casts was observed in 75% of Exp A, 80% of Exp B and 100% of Exp C. Seven Cont F and 9 Cont M were examined extensively for red cell casts. In 3 (43%) of the 7 Cont F and 2 (22%) of the 9 Cont M, red cell cast

**Table 2.** Histopathological findings in the rats of 6 Exps A, B, C, D, E and F (illustrated in figures 1–5).

Exp no (n <sup>*</sup> )	Lung		Liver Embolic n (%)	Intestine Activated LN n (%)
	Red cell cast n (%)	Vessel edema n (%)		
A (4)	3 (75)**	4 (100)	0 (0)	0 (0)
B (5)	4 (80) <sup>†</sup>	5 (100)	3 (60) <sup>‡</sup>	2 (40)
C (4)	4 (100) <sup>§</sup>	4 (100)	0 (0)	1 (25)
D (4)	1 (25)	4 (100)	0 (0)	0 (0)
E (4)	0 (0)	4 (100)	0 (0)	0 (0)
F (5)	1 (20)	5 (100)	1 (20) <sup>§§</sup>	1 (20)

\*Total rat number, \*\*Figures 1a and 2, <sup>†</sup>Fig. 3, <sup>‡</sup>Fig. 4, <sup>§</sup>Increased numbers of vacuoles in type II alveolar cells, <sup>§§</sup>Fig. 5



**Figure 1a.** Light microscopy showing an area of edematous lung in Exp A-1 female rat injected with MASP-2 Ab. Many red cell casts, which suggest the occurrence of complement-activated hemolysis, are demonstrated, around which small red cell fragments are present. At the left side, an edematous arteriole is shown, with edematous adventitia infiltrated by many eosinophils. A part of the arteriolar middle tunic, which is composed of smooth muscle, is damaged. MASP-2 Ab reactions to lung are indicated. Magnification indicated at lower right (H-E stain).

formations were detected sparsely. In the 2 of the 3 Cont F and 1 of the 2 Cont M that had red cell casts, eosinophil infiltration around the blood vessels was also confirmed. Thus, it appears that mild pre-edematous findings such as those illustrated in figure 1a also occur physiologically in relation to eosinophil infiltration even in normal rats. As shown by immunochemical staining in figure 1b, the eosinophil granules contained MASP-2-positive complex antigens. MASP-2 activation must be also triggered by eosinophil granule degradation. Among the Exp A to Exp C rats, in which MASP-2 activation was caused by exogenous MASP-2 Ab injection, rather exceptionally, the Exp A-1 rats (fig. 1a) had eosinophil infiltration. The eosinophils must be destroyed by exogenous MASP-2 Ab in these Exp A to Exp C rats. The electron micrographs shown in figure 2a and figure 2b obtained from an Exp A-2 rat show signs of lung edema. Figure 2a demonstrates an activated large alveolar cell (type II cell). MASP-2 Ab reactions to the type II cell MASP-2 resulted in lamellar body (Lb) secretion and formed many large vacuoles in the cytoplasm, which hinted at the change from type II cell to type I cell. Among Exp A to Exp C rats, the highest vacuole numbers of type II cells were observed in Exp C rat tissue sections followed for 3 days after MASP-2 Ab injection. After heparin sodium had been injected 4 times, heparin sodium induced accelerated

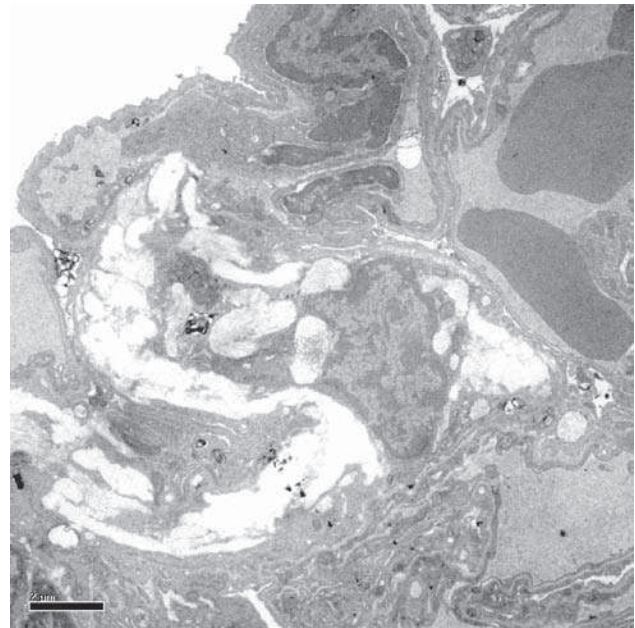


**Figure 2a.** Electron micrograph of lung derived from Exp A-2 female rat injected with MASP-2 Ab. A large type II alveolar cell in the center is surrounded by three bundles of reticular fibers. This cell shows many vacuoles, suggesting that many lamellar bodies (Lb) have already been secreted from the cell. Forepart from one Lb in the center cytoplasm, many small-sized Lb are still present at the edge of the cytoplasm and at center left is an extracellular Lb, which has been secreted from the cell. This figure shows MASP-2 Ab reactions to the type II cell. Magnification indicated at lower left (uranyl acetate-lead citrate double-stain).

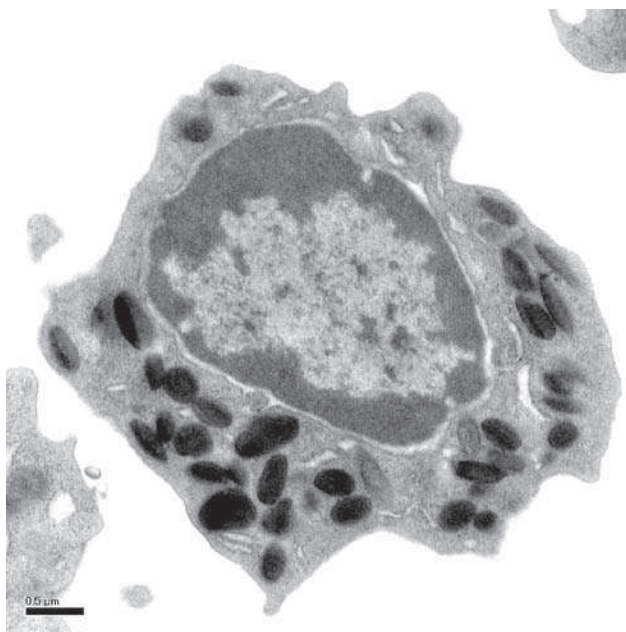


**Figure 1b.** Electron micrograph of BM eosinophil derived from Exp D-3 female rat injected with pTyr mAb. This rat had 78% CD3-positive mesenteric lymph node (MLN) cells at and 91% MASP-2-positive BM cells. Eosinophil granules are stained positively with MASP-2 Ab-gold complexes, many of which have very high density. Eosinophil granules with MASP-2 antigen complexes are recognized. Magnification indicated at the lower left (uranyl acetate-lead citrate double-stain).

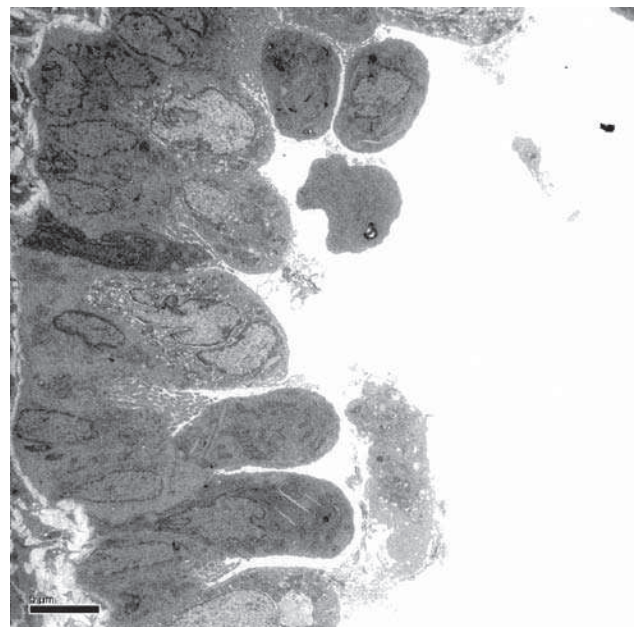


**Figure 2b.** Electron micrograph of lung from Exp A-2 female rat (the same as shown in fig. 2a), showing a bronchiole consisting almost completely of Clara cells, which show active merocrine (apocrine) secretion. Between the apocrine Clara cells, active eccrine secretion is shown. Bronchiole secretion had been reinforced by MASP2 Ab injection. Magnification indicated at lower left (uranyl acetate-lead citrate double-stain).

secretion of lung surfactant (Lb) from type II cells to correct lung damage. Figure 2b shows a part of the bronchiole from an Exp A-2 rat, containing Clara cells, which caused active merocrine secretion. The small bronchioles in these rats were often occupied by a large mass of apocrine-secreted Clara cells. Figures 2a and 2b show characteristic lung edema signs triggered by MASP-2 Ab injection. Exp B rats were injected with both MASP-2 Ab and MHC class I mAb, which triggered lung thrombosis and liver embolism. Figure 3 shows two kinds of lung thrombosis generated at the site of the damaged endothelial cells. The thrombosis shown in figure 3a contains apoptotic leukocytes, platelets and fibrins, which had reacted with MHC class I mAb, and underwent apoptosis. In blood circulation, thrombosis was generated at the site of the damaged endothelial cells. As shown in figure 3b, one of the thromboses has the same characteristics as those of figure 3a, but another small thrombosis contains freshly destroyed red cells, caused not only by MHC class I mAb, but also clearly by MASP-2 Ab. Figure 4 shows a liver embolism found in an Exp B-5 rat. The embolism occupied more than a quarter of one hepatocyte. At the embolic site, ischemic hepatocytes were accompanied by segmented neutrophil infiltration. There is a strong possibility that the embolism shown in figure 4

was caused by a lung thrombosis. Another embolism with more severe apoptotic (lysed) hepatocytes accompanied with bleeding was found with a dilated vein near to the embolism shown in figure 4. The latter embolism has the same pathological findings as those of the Exp F-2 male

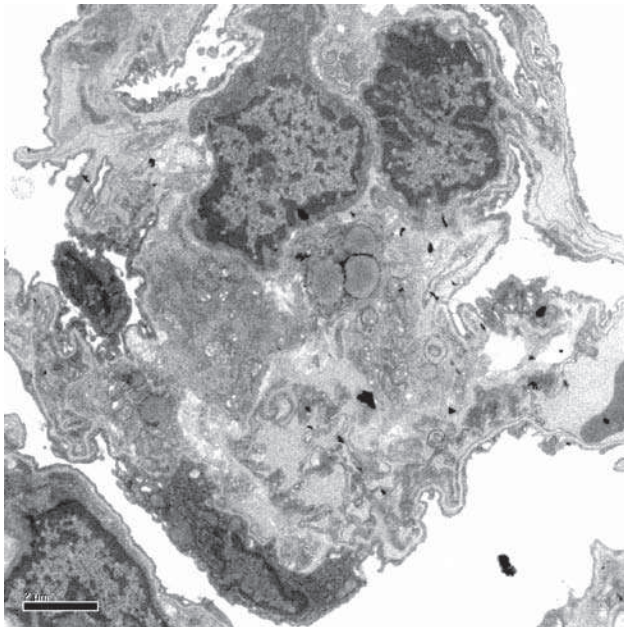


**Figure 3a.** Electron micrograph of a lung thrombosis from Exp B-3 male rat given both MHC class I mAb and MASP-2 Ab. This thrombosis has developed from destroyed endothelial cells, to which dead leukocytes and platelets and fibrins have aggregated. At the upper side, two activated endothelial cells are shown, which indicates that the thrombosis had been formed from the damaged sites by MHC class I mAb and MASP-2 Ab. Magnification indicated at lower left (uranyl acetate-lead citrate double-stain).

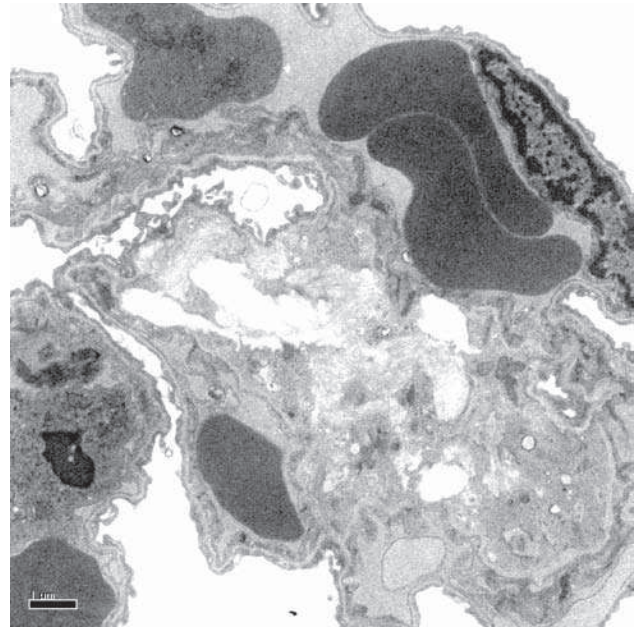


**Figure 3b.** Electron micrograph of lung from Exp B-3 male rat (the same as shown in fig. 3a) showing two kinds of thrombosis. The right large thrombosis has the same characteristics as that in figure 3a. The small left thrombosis contains freshly destroyed erythrocytes, caused by injection of MASP-2 Ab. Magnification indicated at lower left (uranyl acetate-lead citrate double-stain).

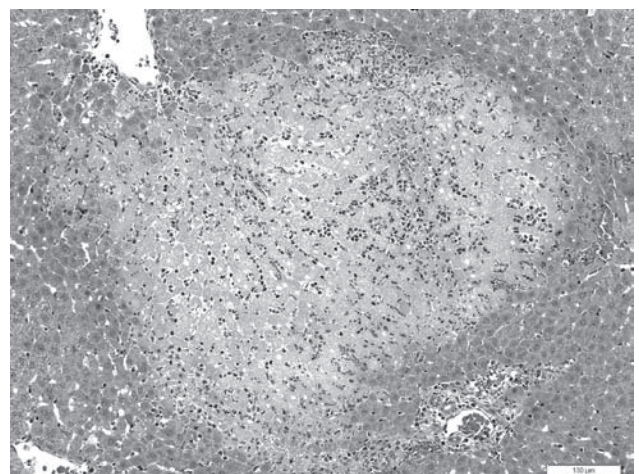


**Figure 4.** Light microscopy of liver from Exp B-5 male rat showing an embolic area. This rat was treated with both MASP-2 Ab and MHC class I mAb. In the embolic area, hepatocytes have undergone ischemic damage accompanied by segmented neutrophil infiltration. At the upper left, a central vein and at the lower right, a portal space are present. Magnification indicated at lower right (H-E stain).

described below, which was caused by liver thrombosis. As the size of the fixed liver samples for tissue section were small, liver embolism was confirmed in only 3 (60%) of the 5 Exp B rats. However, on examination of the whole liver, all the Exp B rats appeared to have had liver embolisms derived from liver thrombosis. At the end of the ileum, the submucosal LN were remarkably enlarged in 40% of Exp B rats and 25% of Exp C rats, based on MASP-2 activation.

The Exp D-Exp E and Exp F rats were injected with pTyr mAs, as shown in table 1. The Exp E rats were given both chemotactic inhibitor and heparin sodium for comparison with the reactions of Exp F males, which were additionally injected with female BM cells. On light microscopy, the liver tissue section of Exp F-2 shows a mass of severely apoptotic (lysed) hepatocytes with bleeding near to a dilated vein, which was judged to be due to a liver embolism caused by liver thrombosis. Exp F rat livers showed sporadic single hepatocyte apoptosis, small focal lymphocyte infiltration and localized venous-bore dilatation. Around the veins, hepatocyte damage was generally more severe in the Exp F rats. Compared with the livers of the Exp E rats, those of the Exp F rats had signs of being affected not only by pTyr mAb but also by immune reactions to injected female BM cells. The electron micrographs shown in figure 5 were obtained from an Exp F-2 rat. Proliferation and degenera-

tion of Golgi apparatuses are observed in the hepatocyte of figure 5a. Small apoptotic hepatocytes retain several degenerated Golgi apparatuses discharged into sinusoidal lumens, as shown in figure 5b. Whole apoptotic hepatocytes were often discharged into sinusoidal cavities and venules, resulting in blockage of the blood flow. In other electron micrographs of the same liver, moderately or markedly edematous adventitia of venules was frequently observed, resulting in narrowing of the vessels.

A small red cell thrombosis containing 4 red cells and 8 red cell fragments in a fibrin net, was detected in the Exp F-2 male liver. In the lung of Cont F3 stained immunohistochemically, the lumen of the Golgi apparatuses contained with pTyr mAb pTyr-Ab-gold complexes, which caused Golgi apparatus damage. Heparin sodium at 30 units per rat had been injected into the Exp E and Exp F rats in both of which its effectiveness could be expected. For erythrocyte, platelet or fibrin thrombosis generated in liver venules, heparin sodium must react to protect the Exp F rats from liver thrombosis and embolism. Ileum LN enlargement in the Exp F-5 rat (20%) was as large as that in 2 (22%) Cont M and 1 (14%) Cont F, but not so much as that found in the MASP-2 Exp B and Exp C rats.

Table 3 shows the FCM results of MLN, BM and lung

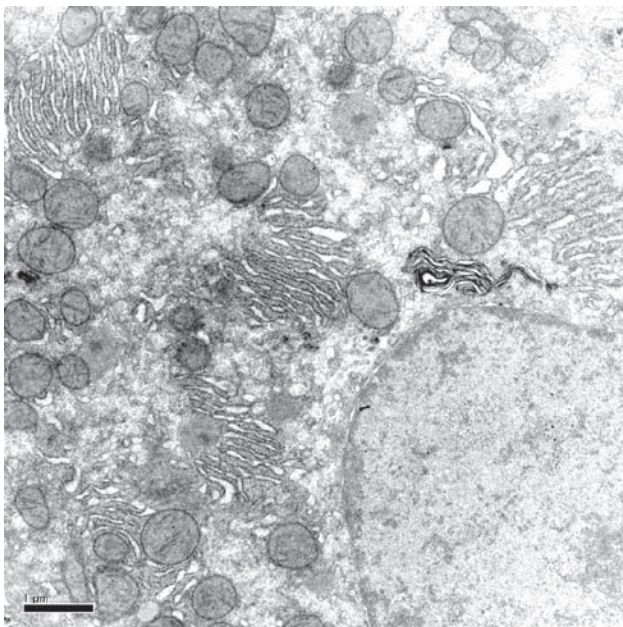


**Figure 5a.** Electron micrograph of an apoptotic hepatocyte from liver of Exp F-2 male rat, with acute GvH reactions due to male-specific mHA after treatments with pTyr mAb, chemotactic inhibitor and female BM cells. The hepatocytes in the apoptotic area are characterized by proliferation of disturbed Golgi apparatuses. Magnification indicated at lower left (uranyl acetate-lead citrate double-stain).

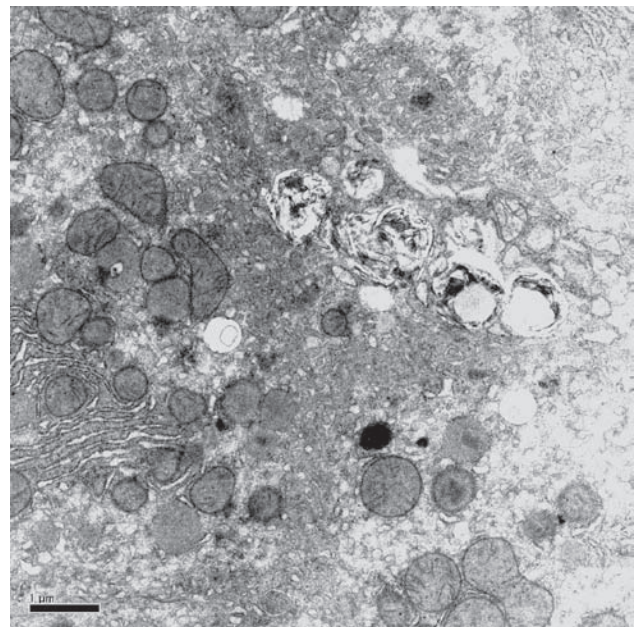


**Figure 5b.** Electron micrograph of liver of Exp F-2 male rat (the same as shown in fig. 5a). Three apoptotic hepatocytes remaining degenerated Golgi apparatuses are shown at the upper right. These apoptotic hepatocytes have been discharged into the sinusoidal lumen (the blood flow of the sinusoidal lumen is often blocked by discharged apoptotic hepatocytes). Magnification indicated at lower left (uranyl acetate-lead citrate double-stain).

**Table 3.** MNC results of MLN, BM and lung samples from the six groups of experimental rats (A, B, C, D, E, F) and control rats (Cont) treated with either MASP-2 Ab or pTyr mAb (illustrated in figures 6–7).

Exp no (Sex)	Total rats (n*)	MLN (%)		BM (%)		Lung (%)
		CD3+	CD8a +	MASP-2 +	pTyr +	MASP-2+
A (F)	4	71±2	NT**	NT	NT	95±8
B (M)	5	71±1	NT	99±1	NT	92±2
C (M)	4	78±2	NT	95±3	95±2	93±1
D (F)	4	82±6	NT	87±3	NT	68±2
E (F)	4	74±3	18±0.2	45±12	61±10	83±5
F (M) <sup>†</sup>	4	68±2	15±1	78±8	27±3	79±4
	1 <sup>‡</sup>	79	23	78	26	80
Cont (F)	7	76±3	15±1 <sup>§</sup>	99±1 <sup>§§</sup>	97±2 <sup>§§</sup>	95±4
Cont (M)	7	71±2	15±1	95±6	95±5	98±1

\*Total rat number, \*\*Not tested, <sup>†</sup>GvHD, <sup>‡</sup>Exp F-3 rat, <sup>§</sup>N=3, <sup>§§</sup>N=5

preparations, which were stained with FITC-conjugated CD3, CD8a, MASP-2 and pTyr mAbs or Ab. In the MLN of Exp D rats that had been injected with pTyr mAb, the CD3-positive cell % was slightly increased to 82±6%. B cell numbers decreased slightly in the Exp D rats. Slightly increased CD8a-positive cells were present in the Exp E rats (18±0.2%) showing 74±3% of CD3-positive MLN cells. Cont F showed 76±3% of CD3-positive MLN cells. Chemokine inhibitor of Exp E rats suppressed CD3-positive MLN cells to 74±3%, from 82±6% found in the Exp D rats without chemotactic inhibitor. Exp F-3 male showed increased CD8a-positive cells in the MLN (23%). The Exp F-3 male had about 50% apoptotic non-lymphocytes in the MLN, and depleted host lymphocyte numbers in the MLN and spleen. Four other Exp F males showed a slightly low % of CD3-positive T cells (68±2%), but no decrease of CD8a-positive cells (15±1%). Thus, in addition to T cell depletion in the MLN, there was a relative increase of CD8a-positive cells in the T cells. Exp F-2, 3 and 5 rats had BW gains of 40 g, 38 g and 42 g, 16 days respectively after the start of the experiment, while the gain for Exp F-1 and 4 rats was 58 g and 71 g, respectively, so the first 3 rats had suppressed BW gain. From the results of FCM of MLN, the Exp F rats were judged to have undergone variable degrees of GvH reaction. Chemotactic inhibitor at 150 µg/rat acted to reduce the signs of GvH reaction. Host lymphocyte depletion from the LN was protected from GvH reaction by chemotactic inhibitor in the Exp F rats, except for the Exp F-3 rat, in which chemotactic inhibitor must react more poorly.

The FCM results of lung MNC stained with MASP-2 Ab conjugated with FITC are demonstrated in figure 6a. MASP-2 antigen was expressed in both type I and type II alveolar cells. The highest % of MASP-2-positive cells was detected in Exp A-3 (97%), which had been injected with MASP-2

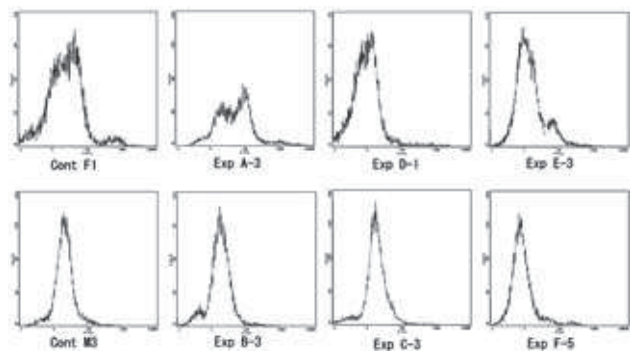


**Figure 6a.** FCM of lung sample stained with FITC-conjugated MASP-2 Ab. A fixed border point between negative and positive peaks was confirmed using results such as those for Exp A-3, Exp B-3 and Exp C-3. MASP-2-positive cell percentage of each rat is 88% (Cont F1), 97% (Exp A-3), 69% (Exp D-1), 89% (Exp E-3), 96% (Cont M3), 92% (Exp B-3), 92% (Exp C-3) and 73% (Exp F-5). MASP-2 Ab injection into Exp A, B and C rats did not suppress expressions of lung MASP-2. However, pTyr mAb injection into Exp D, E and F rats suppressed expressions of lung MASP-2 (tab. 3).

Ab. Exp B-3 and Exp C-3 rats, which were also injected with MASP-2 Ab, showed 92% MASP-2-positive cells in both rats. However, in the 3 rats Exp D-1, Exp E-3 and Exp F-5, which were injected with pTyr mAb, the MASP-2-positive cells were 69%, 89% and 73%, respectively. Apart from the Exp E-3 rat which had exogenous chemotactic inhibitor, Exp D-1 and Exp F-5 rats exhibited more suppressed MASP-2 expression in their lungs. Table 3 summarizes the FCM results of MLN, BM and lung preparations from the rats treated with either MASP-2 Ab or pTyr mAb. Exp D, Exp E and Exp F rats exhibited suppressed expression of MASP-2-positive cells (68±2% to 83±5%), while Exp A, Exp B and Exp C rats, which had received MASP-2 Ab, had MASP-2-positive cells at 92±2% to 95±8%. Lung MASP-2 expression was suppressed by pTyr mAb. Exp D rats, without chemotactic inhibitor, exhibited suppressed expression

(68±2%) of MASP-2-positive lung cells, but Exp E and Exp F rats, with chemotactic inhibitor, showed more mild suppression of MASP-2-positive lung cells. Compared with that of Exp E rats (83±5%), Exp F rats had lower expression of lung MASP-2 (79±4%). It was concluded that chemotactic inhibitor protected Exp E and Exp F rat lungs from MASP-2 suppression, with the help of heparin injections. Figure 6b

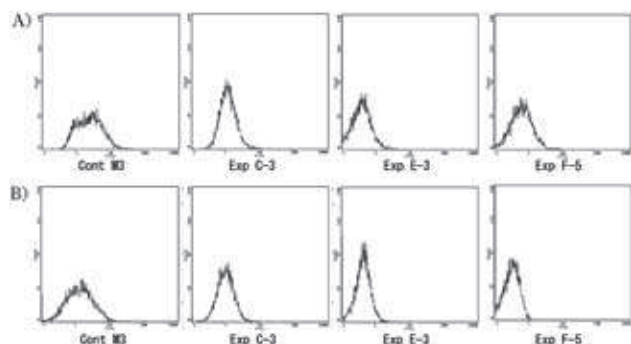


**Figure 6b.** FCM of BM stained with FITC-conjugated MASP-2 Ab stage A, and FITC-conjugated pTyr mAb in stage B. A fixed border point between MASP-2-positive and -negative peaks was decided by the result of control rat Cont M3. The MASP-2-positive cell percentage was 99% (Cont M3), 98% (Exp C-3), 41% (Exp E-3) and 68% (Exp F-5) at stage A. The results of pTyr-positive cells were followed to the MASP-2 border point. PTyr-positive cell % at stage B was 90% (Cont M3), 93% (Exp C-3), 53% (Exp E-3) and 29% (Exp F-5) in the same rats shown for stage A. The Exp C-3 rat was treated with MASP-2 Ab, and the Exp E-3 and Exp F-5 rats were treated with pTyr mAb.

shows the BM FCM results, stained with FITC-conjugated MASP-2 Ab or with FITC-conjugated pTyr mAb, in the same rats, Exp C-3, Exp E-3 and Exp F-5. In the Exp C-3 rat given MASP-2 Ab, as for the lung FCM, the BM MASP-2-positive cells were 98% and BM pTyr-positive cells were 93%. Exp E-3 and Exp F-5 rats were given pTyr mAb, and, as expected in the lung FCM results, MASP-2-positive BM cells were at low levels of 41% and 68% in both the rats, and pTyr-positive BM cells were 53% and 29%, respectively. As shown in table 3, the values of both MASP-2-positive and pTyr-positive BM cells were high in the rats injected with MASP-2 Ab, but low in the rats injected with pTyr mAb. The Exp E rats showed lower values of BM MASP-2-positive cells (45±12%) than expected, but those of BM pTyr-positive cells were the theoretical values of 61±10%. All the Exp F rats had pTyr-positive BM cells at numbers of lower than 30%. BM cell activation of the Exp F rats was further restricted by donor cell rejection. GvH reaction in the liver, MLN and BM was aggravated by the injection of pTyr mAb. The suppression of pTyr in host cells led to donor cell activation. It was concluded that in Exp F using male hosts, female BM donor cells rejected host male-specific mHA derived from their father.

The lung electron micrographs in figure 7 show high-density granules of MASP-2 antigens stained with MASP-2 Ab-gold complexes. The type I alveolar cell of figure 7a

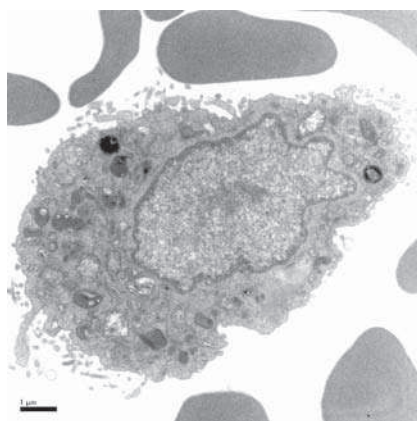


**Figure 7a.** Electron micrograph of a squamous alveolar cell (type I cell) derived from a control female rat (Cont F3), stained with MASP-2 Ab-gold before fixing (immunochemical stain). In the upper left part of the cytoplasm, a MASP-2-positive site is shown as a high-density round granule, with a pair of close-by centrioles. At the upper right another granule stained with MASP-2 Ab-gold is also seen. Magnification indicated at lower left (uranyl acetate-lead citrate double-stain).

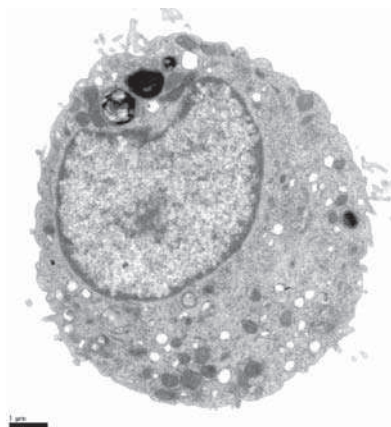


**Figure 7b.** Electron micrograph of a squamous alveolar cell derived from Exp C-3 male rat, which had been given MASP-2 Ab, followed for 3 days with heparin. The lung cell suspension was stained with MASP-2 Ab-gold before fixing. Compared with control lung cells (fig. 7a), the granule of MASP-2 Ab-gold complexes was larger (i.e., activated) in the Exp C-3 rat. Two small granules positive for MASP-2 Ab-gold are also observed. To the left of the two MASP-2-positive granules, a destroying MASP-2-positive granule that must have reacted with MASP-2 Ab is present. Magnification indicated at lower left (uranyl acetate-lead citrate double-stain).

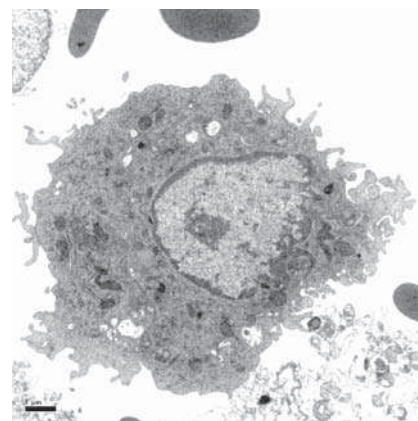


**Figure 7c.** Electron micrograph of a squamous alveolar cell is derived from Exp D-2 female rat which had been given pTyr mAb. The lung cell suspension was stained with MASP-2 Ab-gold before fixing. Compared with those of cells from control rat (Cont F3, shown in fig. 7a), two very tiny MASP-2-positive granules are seen at the upper right and under left sides of near to nucleus. The mitochondrial membranes are stained non-specifically, but more strongly, with this immunochemical staining than those of Cont F3. Magnification indicated at lower left (uranyl acetate-lead citrate double-stain).

is derived from Cont F3 rat. The type I cell of figure 7b is derived from Exp C-3 rat injected with MASP-2 Ab and the type I cell of figure 7c is derived from Exp D-2 rat injected with pTyr mAb. All the 3 cells were squamous alveolar cells without Lb. MASP-2 Ab injection did not lead to the suppression of MASP-2, while pTyr mAb injection led to suppressed expression of MASP-2, as shown in FCM. MASP-2 antigens destroyed by MASP-2 Ab were recovered quickly by activated expression of another MASP-2. When MASP-2 antigen was suppressed by pTyr mAb, mitochondrial membranes were stained non-specifically with MASP-2 Ab-gold complexes. In particular, in BM cells, MASP-2 Ab-gold complexes were actively taken up in the mitochondrial membranes, when they were attacked by pTyr mAb. In the Exp E BM cells, mitochondrial membranes must have remained relatively normal, as reflected by the low MASP-2 values ( $45 \pm 12\%$ ) of Exp E BM cells. It is possible that MASP-2 Ab-gold complexes did not indicate single MASP-2, even when stained positively with MASP-2 Ab. However, when a granule was stained positively with MASP-2 Ab, it is certain that the granule contained MASP-2-positive antigens to react to MASP-2 Ab.

## DISCUSSION

The MASP-2 polypeptide chain has 686 amino acid (aa) residues, including a 15 aa single peptide. One mutated MASP-2 had a substitution of glycine for aspartic acid at aa 120 in the CUB1 domain found in CC1r/CC1s, Uegf and bone morphogenic protein 1. In association with the low levels of both MASP-2 and a short splice product of MASP-2 (MAP19), and severe hypocomplementemia with anti-C1q autoantibodies and low C1q levels, were detected in this mutated case.<sup>6</sup> As the mutated MASP-2 failed to bind to MBL, a severe pneumococcal infection which developed was suspected to be due to MASP-2 insufficiency. In the 2000s, at least 7 types of naturally occurring polymorphisms of MASP-2 have been reported: R99Q, D120G and P126L in the N-terminal CUB1 domain, H155R and CHNHdup (4 aa duplication; CHNH 156–159 to dupCHNH 160–163) in the EGF domain (a  $\text{Ca}^{2+}$ -binding epidermal growth factor-like domain), V377A in the second CCP domain and R439H in the activation peptide section.<sup>7</sup> When MASP-2 is activated, the polypeptide chain is cleaved at the arginine (R444)-isoleucine (I445) peptide bond (between the activation peptide and the remainder of the serine protease domain), resulting in two fragments, the A chain and B chain. Following this, C434 in the activation peptide and C552 in the serine protease domain are held together with a disulfide bond. A new structure of MASP-2 is formed in the activation. Apart from D120G and CHNHdup, which cannot associate with MBL and induce C4 fragment deposition,

the other polypeptides bind well to MBL. The R439H variant is deficient in cleaving C4, despite its normal binding to MBL. R439H gene frequency was estimated to be 9%. Generally, MASP-2 polymorphisms were not rare genotypes in humans.

In this animal study using rats, MASP-2 Ab injection, caused MASP-2 activation, as confirmed by FCM and electron micrography. The new structure of activated MASP-2 described above, which had been formed in this study, must have cleaved C4 efficiently. Although MLN activation was observed in the submucosal LN on the basis of MASP-2 activation, acute lung infection due to MASP-2 insufficiency was not triggered. Rather than lung infection, intraalveolar edema and increased peribronchovascular edema were induced by secondary activated MASP-2.

Pulmonary surfactant protein-A (SP-A) has a similar domain structure and architecture to MBL, but lacks any intrinsic complement activity. SP-A cannot bind to MASP-2 and cannot activate complement, although MASP binding of SP-A can be easily engineered through 3 aa substitutions to the collagenous domain of MBL.<sup>8</sup> The MASP-binding site in MBL and ficolins is characterized by a distinct motif within the collagenous domain: Hyp (hydroxyproline)-Gly-Lys-Xaa (aliphatic residue)-Gly-Pro. In SP-A, Glu, Cys and Glu were replaced by lysine, leucine, and proline residues, respectively, to establish new MASP binding, in which the lysine was essential for binding. Pulmonary surfactant stored in Lb is a complex mixture of lipids (phospholipids) and proteins (surfactant apoproteins), which forms a lining layer at the air-liquid interface. It has been reported that intratracheal administration of exogenous surfactant decreased intraalveolar edema formation and the development of atelectases, and, especially, peribronchovascular edema.<sup>9</sup> The MASP-2 Ab in this study was justified to be directly responsible for increased permeability of the blood-air barrier. In addition to complement-dependent air-liquid interface damage, simultaneously activated pTyr signal pathways were associated with the acute transient lung damage. As found in the Lb-empty large vacuoles of activated type II cells, fusion-activated  $\text{Ca}^{2+}$  entry (FACE), which occurred at the time of Lb-plasma membrane fusion, enhanced surfactant release from type II cells in an actin-dependent process.<sup>10</sup> Activated apocrine secretion from bronchiolar Clara cells could be explained as being initiated by mediators interacting with RTK activating phospholipase C (PLC), as mediated by G protein-coupled receptor (GPCR) signals.<sup>11</sup> Increased apocrine secretion of Clara cells, as occurs in asthma, was an indirect indication of the acute lung edema in these rats injected with MASP-2 Ab.

Eosinophil granulocytes are found in the respiratory

mucosa, the gastrointestinal tract and lymphocyte-associated organs. Elevated eosinophil cationic protein (ECP), which is the best known basic protein in eosinophil granules, is found in T helper lymphocyte type 2 diseases, such as allergic asthma and allergic rhinitis.<sup>12</sup> ECP is a peptide of 133 aa with the first 40 aa necessary for membrane interfering heparin binding and cytotoxic activity. However, the mast cell products and eosinophil major basic protein (MBP) are correlated to a greater degree with bronchial hyperactivity. In this study, eosinophils were often found infiltrated in the rat lungs with pre-edematous changes of bronchial hyperactivity. Mast cell proliferation was observed in the lung edema. The intestinal LN were enlarged in the MASP-2 rats and the eosinophil granules stained positively with MASP-2 Ab. In this study, MASP-2-positive complexes of eosinophil granules were explained as follows: Firstly, rat ficolin-B in the eosinophil granules was set up for the MASP-2 binding. Rat ficolin-B corresponds to human M-ficolin, although rat ficolin-A corresponds to human L-ficolin. Recently, rat ficolin-B has been reported to have activated MASP-2 in a manner comparable to that of ficolin-A, although the activation was half that of ficolin-A.<sup>13</sup> It was therefore concluded that the MASP-2 complexes in the eosinophil granules that stained positively with MASP-2 Ab must be ficolin-B-MASP-2 complexes.

In this study, lung thrombosis formation was prominent when MHC class I mAb was injected together with MASP-2 Ab. Serine protease inhibitor antithrombin III (AT-III) was judged not to be low in these MASP-2 Ab rats because serine protease activity should be high in these rats. Furthermore, MASP-2 activation, which has factor Xa-like activity and activates thrombin, must have led to fibrin clot formation in these MASP-2 rats.<sup>2,14</sup> Heparin inhibits MASP-1 and -2 and thrombin activities together with AT-III. Heparin sodium is therefore expected to react effectively to prevent fibrin clot formation, which involves thrombosis. Although clinical hemolytic events are more apparent than thrombosis in the MASP-2 rats injected with heparin, it was correct that, as a whole, small amounts of heparin sodium injection acted effectively to prevent the hypercoagulopathy induced by MASP-2 activation. Active vacuole formation of type II cells, which reflected active secretion of lung surfactant, was recognized in the MASP-2 rats injected with heparin to repair injured lung tissue. Heparin injection was absolutely necessary as an effective anticoagulant, when MHC Abs were detected in addition to MASP-2 Ab.

The rats injected with pTyr mAb, which showed suppressed expressions of MASP-2 and pTyr in FCM, exhibited a liver type of FL-Ron RTK (deleted SF-Ron PTK).<sup>3</sup> In the

experimental rats that received pTyr mAb, splenocytes might have had a greater production of IFN- $\gamma$ .<sup>3</sup> Kupffer cells might have produced high levels of tumor necrosis factor alpha (TNF- $\alpha$ ), like the Ron RTK-/- type.<sup>15</sup> In this study, acute severe liver injury was not observed, but cytokine-induced moderate liver injury was seen in the rats with pTyr mAb injection, the hepatocytes of which had accelerated apoptosis with impaired Golgi apparatus. Chemotactic inhibitor, peoniflorin (PF), has been reported to have anti-inflammatory capacity against TNF- $\alpha$ -induced chemokine production in human dermal microvascular endothelial cells by blocking nuclear factor- $\kappa$ B (NF- $\kappa$ B) and extracellular signal-regulated kinase (ERK) 1/2 pathways.<sup>16</sup> As macrophage chemoattractant protein-1 (MCP-1), macrophage inflammatory protein-2 (MIP-2), interleukin-1 receptor antagonist (IL-1ra), IL-6, keratinocyte chemoattractant (KC), and tissue inhibitor of metalloproteinase (TIMP-1) have previously been reported to be elevated in the media from Ron RTK-/- cells, in these rats with pTyr mAb, chemotactic inhibitor was judged to have reacted effectively to suppress cytokine-induced chemokine reactions.<sup>15</sup>

Judging from the results of suppressed MASP-2 and pTyr expressions of BM cells, the B and myeloid cells of the experiment rats injected with pTyr mAb might also have disturbed functions. B cell and myeloid cell development has been found to require Bruton tyrosine kinase (Btk) in a mouse model.<sup>17</sup> Neutrophil migration is significantly reduced in Btk-deficient animals with enhanced granulopoiesis in the BM. Human mutation in the Bruton tyrosine kinase (BTK) gene causes X-linked agammaglobulinemia (XLA). BTK-deficient B cells lead to a complete loss of peripheral B cells. On the other hand, male-specific genes are located on the nonrecombining region of the Y chromosome. Epitopes of male-specific mHA are identified as immunogens that cause GvHD. DBY, a model of male-specific mHA revealed a high CD4-positive T cell response in a male recipient of transplanted BM cells from a human histocompatibility leukocyte antigen (HLA)-identical female sibling.<sup>18</sup> After transplant, the patient developed very high reactivity to the 19-mer peptide DBY<sub>30-48</sub>, which persisted from 8 to 21 months post-transplantation. The antibody responses were mapped to 2 DBY peptides at positions 118–134 maximally at 16 months after transplant and 536–552 maximally at 21 months after transplant, which indicated that antibody response to DBY evolved by targeting a new DBY epitope. In this study, host male-specific mHA received pTyr mAb was rejected by female donor cells, in which leukocytes had impaired motility.<sup>4,17</sup> Atypical acute GvHD due to male-specific mHA was recognized mildly or moderately in the Ron RTK deficient-like rats.

It was also suspected that activated coagulation factor XIII (FXIIIa) must have been affected in this study by reduced tyrosine kinase-dependent actions.<sup>19</sup> FXIIIa works to stabilize fibrin clot and on the platelet surface plays a role in the development of highly procoagulant-coated platelets. Platelets usually bind to FXIII through  $\alpha_{IIb}\beta_3$  integrins, which requires tyrosine kinase-dependent signals, in a potentially collaborative binding of  $\alpha_v\beta_3$ . In the rats treated with pTyr mAb, FXIIIa involved in a down-regulated tyrosine kinase mechanism, and instead, bound to platelets

through catalytic A-subunits of FXIII (FXIII-A). Low levels of MASP-2 did not split FXIII and platelets actively.<sup>2</sup> FXIIIa supported more strongly platelet activation and enhanced thrombosis formation, together with subendothelial matrix proteins, such as collagen and von Willebrand factor (VWF), under blood flow conditions. Apoptotic hepatocytes discharged into venous sinusoids blocked blood flow in these experimental rats with GvH reactions, which had an accelerating influence upon thrombosis formation.

## ΠΕΡΙΛΗΨΗ

**Πνευμονικό οίδημα και θρόμβωση που προκαλούνται από ενεργοποίηση αντιδράσεων με MBL σε συνδυασμό με MASP-2 και αντιδράσεων του MHC τάξης I, καθώς και ηπατική θρόμβωση προκαλούμενη από αντιδράσεις καταστολής της φωσφοτυροσίνης σε θήλεις δότες και ειδικά αντιγόνα σε άρρηνες αρουραίους Lewis**

T. NAKATSUJI

*Department of Transfusion Cell Therapy, Hamamatsu University School of Medicine, Hamamatsu 431-3192, Ιαπωνία*

*Αρχεία Ελληνικής Ιατρικής 2011, 28(5):680–691*

**ΣΚΟΠΟΣ** Διερεύνηση του πνευμονικού οιδήματος και της θρόμβωσης, καθώς και του ηπατικού εμβολισμού. **ΥΛΙΚΟ ΚΑΙ ΜΕΘΟΔΟΣ** Χρησιμοποιήθηκαν ποντίκια Lewis. Για την πρόκληση πνευμονικού οιδήματος χορηγήθηκε MBL (mannose-binding lectin) σε συνδυασμό με αντίσωμα MASP-2 (serine protease 2). Η θρόμβωση πνευμόνων και ήπατος, καθώς και ο εμβολισμός, προκλήθηκαν με τη χρήση μονοκλωνικού αντισώματος (mAb) κατά του MCH τάξης I και αντισώματος κατά της MASP-2. Οι εμβολισμοί του ήπατος ευοδώθηκαν με mAb φωσφοτυροσίνης (pTyr) και αντιδράσεις ειδικών αντιγόνων κατά ελασσόνων αντιγόνων ιστοσυμβατότητας (mHA). Οι σχετικές εκφράσεις της MASP-2 και της pTyr επιβεβαιώθηκαν με κυτταρομετρία ροής (FCM). **ΑΠΟΤΕΛΕΣΜΑΤΑ** Το αντίσωμα κατά της MASP-2 προκάλεσε οξύ ενδοκυψελιδικό και περιβρογχοαγγειακό οίδημα, με χαρακτηριστικά ευρήματα αιμολυτικών ερυθροκυτταρικών κυλίνδρων, κυτταρική ενεργοποίηση τύπου II με έκκριση μεμβρανικών σωμάτων (Lb) και αυξημένη αποκρινική έκκριση των κυττάρων Clara. Το mAb κατά του MHC τάξης I και το Ab κατά της MASP-2 προκάλεσαν βαριά θρόμβωση πνεύμονα και ήπατος, καθώς και εμβολισμό. Οι ανοσοϊστοχημικά χρωματισμένες μικροφωτογραφίες ηλεκτρονικού μικροσκοπίου των κυψελιδικών κυττάρων τύπου I έδειξαν μια άλλη ταχεία ενεργοποίηση της MASP-2, ενώ η άλλη MASP-2 καταστράφηκε από το Ab κατά της MASP-2. Στο ήπαρ όπου ενέθηκε αντίσωμα κατά της pTyr, τα ηπατοκύτταρα παρουσίασαν εκλεκτική απόπτωση με διαταραχές της συσκευής Golgi. Η θρόμβωση του ήπατος που επιβαρύνθηκε από απόρριψη του θήλεος δότη από τα ειδικά mHA του άρρηνος, συνδυαζόταν με διάταση των ηπατικών φλεβών. Η νατριούχος ηπαρίνη αύξησε την έκκριση πνευμονικού επιφανειοδραστικού παράγοντα (surfactant, Lb). Ο χημειοτακτικός αναστολέας κατέστειλε τις χημειοκίνες, οι οποίες προάγονται από κυτταροκίνες που αυξήθηκαν από το Ab κατά της pTyr. **ΣΥΜΠΕΡΑΣΜΑΤΑ** Πνευμονικό οίδημα και θρόμβωση προκαλούνται από τα αντισώματα κατά της MASP-2 και κατά των αντιγόνων του MHC τάξης I. Η χορήγηση mAb κατά της pTyr mAb αύξησε την ηπατική θρόμβωση λόγω διαταραχών της τυροσινικής κινάσης, στην οποία οι ανοσιακές αντιδράσεις κατά του mHA συνοδεύονται από αυξημένη ηπατική θρόμβωση.

**Λέξεις ευρητηρίου:** Εμβολισμός ήπατος, Mannose-binding lectin (MBL)-associated serine protease 2, Πνευμονική θρόμβωση, Πνευμονικό οίδημα, Τυροσινική κινάση

## References

- HARMATV, GÁL P, KARDOS J, SZILÁGYI K, AMBRUS G, VÉGH B ET AL. The structure of MBL-associated serine protease-2 reveals that identical substrate specificities of C1s and MASP-2 are realized through different sets of enzyme-substrate interactions. *J Mol Biol* 2004, 342:1533–1546
- KRARUP A, WALLIS R, PRESANIS JS, GÁL P, SIM RB. Simultaneous activation of complement and coagulation by MBL-associated serine protease 2. *PLoS One* 2007, 2:e623
- WETZEL CC, LEONIS MA, DENT A, OLSON MA, LONGMEIER AM, NEY PA ET AL. Short-form Ron receptor is required for normal IFN- $\gamma$  production in concanavalin A-induced acute liver injury. *Am J Physiol Gastrointest Liver Physiol* 2007, 292:G253–G261
- KITADA T, MIYOSHI E, NODA K, HIGASHIYAMA S, IHARA H, MATSUURA N ET AL. The addition of bisecting N-acetylglucosamine residues to E-cadherin down-regulates the tyrosine phosphorylation of  $\beta$ -catenin. *J Biol Chem* 2001, 276:475–480
- NAKATSUJI T. Complete regeneration of the pancreas including islets of Langerhans, acinar cells, centro-acinar cells, intercalated duct cells, and secretory duct cells in Lewis rats. *Arch Hellen Med* 2011, 28:89–102
- STENGAARD-PEDERSEN K, THIEL S, GADJEVA M, MØLLER-KRISTENSEN M, SØRENSEN R, JENSEN LT ET AL. Inherited deficiency of mannan-binding lectin-associated serine protease 2. *N Engl J Med* 2003, 349:554–560
- THIEL S, KOLEV M, DEGN S, STEFFENSEN R, HANSEN AG, RUSEVA M ET AL. Polymorphisms in mannan-binding lectin (MBL)-associated serine protease 2 affect stability, binding to MBL, and enzymatic activity. *J Immunol* 2009, 182:2939–2947
- GIRIJA UV, FURZE C, TOTH J, SCHWAEBLE WJ, MITCHELL DA, KEEBLE AH ET AL. Engineering novel complement activity into a pulmonary surfactant protein. *J Biol Chem* 2010, 285:10546–10552
- DREYER N, MÜHLFELD C, FEHRENBACH A, PECH T, VON BERG S, NAGIB R ET AL. Exogenous surfactant application in a rat lung ischemia reperfusion injury model: effects on edema formation and alveolar type II cells. *Respir Res* 2008, 9:5
- MIKLAVC P, FRICK M, WITTEKINDT OH, HALLER T, DIETL P. Fusion-activated  $Ca^{2+}$  entry: an “active zone” of elevated  $Ca^{2+}$  during the postfusion stage of lamellar body exocytosis in rat type II pneumocytes. *PLoS One* 2010, 5:e10982
- ABDULLAH LH, DAVIS CW. Regulation of airway goblet cell mucin secretion by tyrosine phosphorylation signaling pathways. *Am J Physiol Lung Cell Mol Physiol* 2007, 293:L591–L599
- BYSTROM J, AMIN K, BISHOP-BAILEY D. Analysing the eosinophil cationic protein – a clue to the function of the eosinophil granulocyte. *Respir Res* 2011, 12:10
- GIRIJA UV, MITCHELL DA, ROSCHER S, WALLIS R. Carbohydrate recognition and complement activation by rat ficolin-B. *Eur J Immunol* 2011, 41:214–223
- GULLA KC, GUPTA K, KRARUP A, GAL P, SCHWAEBLE WJ, SIM RB ET AL. Activation of mannan-binding lectin-associated serine proteases leads to generation of a fibrin clot. *Immunology* 2009, 129:482–495
- STUART WD, KULKARNI RM, GRAY JK, VASILIAUSKAS J, LEONIS MA, WALTZ SE. Ron receptor regulates Kupffer cell-dependent cytokine production and hepatocyte survival following endotoxin exposure in mice. *Hepatology* 2011, 53:1618–1628
- CHEN T, GUO Z, JIAO X, JIA R, ZHANG Y, LI J ET AL. Peoniflorin suppresses tumor necrosis factor- $\alpha$  induced chemokine production in human dermal microvascular endothelial cells by blocking nuclear factor- $\kappa$ B and ERK pathway. *Arch Dermatol Res* 2011, 303:351–360
- FIEDLER K, SINDRILARU A, TERSZOWSKI G, KOKAI E, FEYERABEND TB, BULLINGER L ET AL. Neutrophil development and function critically depend on Bruton tyrosine kinase in a mouse model of X-linked agammaglobulinemia. *Blood* 2011, 117:1329–1339
- ZORN E, MIKLOS DB, FLOYD BH, MATTES-RITZ A, GUO L, SOIFFER RJ ET AL. Minor histocompatibility antigen DBY elicits a coordinated B and T cell response after allogeneic stem cell transplantation. *J Exp Med* 2004, 199:1133–1142
- MAGWENZI SG, AJJAN RA, STANDEVEN KF, PARAPIA LA, NASEEM KM. Factor XIII supports platelet activation and enhances thrombus formation by matrix proteins under flow conditions. *J Thromb Haemost* 2011, 9:820–833

### Corresponding author:

T. Nakatsuji, Department of Transfusion Cell Therapy, Hamamatsu University School of Medicine, 1-20-1 Handayama, Higashi-ku, Hamamatsu 431-3192, Japan  
e-mail: nh80415@hama-med.ac.jp